Strength, stability and size effects in the brittle behaviour of bonded joints under torsion: theory and experimental assessment

N. PUGNO and A. CARPINTERI

Department of Structural Engineering, Politecnico di Torino, Torino, Italy

Received in final form 19 July 2001

ABSTRACT This paper describes a simple Griffith fracture energy criterion to predict the brittle failure load for tubular or non-tubular bonded joints subjected to torsion. The theoretical solution generalizes to non-tubular bonded joints an analogous result already presented in the literature and experimentally validated for particular tubular bonded joints. The stability of brittle crack propagation and the size effects on mechanical collapse behaviour, as well as the ductile–brittle transition, are analysed. Experimental measurements of failure loads under torsion for non-tubular bonded joints agree satisfactorily with the theoretical predictions.

Keywords bonded joints; brittle collapse; non-tubular; size effects; stability; torsion; tubular.

INTRODUCTION

With the development of high-strength adhesive materials and with the progress in techniques of adhesive bonding, various kinds of adhesive-bonded joints are now being used in the manufacturing of light structures. As stress concentration often occurs in the edge zones of the adhesive layer of a joint a detailed analysis of the stress distribution around the joint region, especially in the adhesive layer of these joints, as well as of the brittle behaviour of the joint, is needed for application and research.

Since the pioneering papers by Goland and Reissner,[1] Lubkin and Reissner[2] and more recently by Adams and Peppiatt,[3] several theoretical, numerical and experimental analysis on tubular bonded joints have been performed.

It is only recently that non-tubular structures have been investigated. Pugno and Surace[4] studied a non-tubular joint subjected to torsion from a theoretical point of view and validated it numerically by a three-dimensional finite element analysis. An extension considering tapered adherends has been also presented.[5] Pugno[6] and Pugno and Surace[7] have considered the non-tubular and tubular joint as streamlined for uniform torsional strength (*uts*): starting from a non-tapered joint, the optimization was achieved by chamfering the edges, which are in any case not involved in the stress flow induced by the load for which the joint should be designed. The resulting optimized joint shape is thus both lighter and stronger.

In the present paper a simple study to predict the brittle failure load for a tubular or non-tubular bonded joint under torsion is presented. It is assumed that all three of the materials making up the joint (beams and adhesive) are governed by a linear elastic law (isotropic). Although this is intuitively obvious for beams (which typically are metallic), this is not the case for the adhesive, which is more likely to show a non-linear behaviour. However, if the adhesive film is considered to be under torsion (tubular joint) and not subject to tension, the statistical theory of the rubber[8] shows how its behaviour can be considered to be substantially linear elastic. On the contrary, in the case of a non-tubular joint, the stress state in the adhesive is basically normal. As is well known, the adhesive can withstand shear stresses which are an order of magnitude higher than the ultimate normal stresses, so that we can also assume a linear elastic law for the adhesive of a non-tubular joint.

A very general formula has been obtained by means of the Griffith[9] energy balance and applying linear elastic fracture mechanics.[10–16] It is supposed that the crack propagation at the interface between the two adherends

Correspondence: Nicola Pugno, Department of Structural Engineering, Politecnico di Torino, Corso Duca degli Abruzzi 24, 10129 Torino, Italy.
E-mail: pugno@polito.it

takes place in the adhesive at the point of highest stress concentration in Mode I.[8] An energy balance is formulated for a small growth of the debonding: changes in the strain energy of the joint and in the potential energy of the loading device are equated to the characteristic energy needed for debonding. As a consequence a general formula to predict the brittle failure load for a tubular or non-tubular bonded joint with or without tapered adherends can be obtained. This formula generalizes an analogous formula already presented in the literature[8] and experimentally validated for tubular bonded joints. The greater sensitivity to brittle collapse is emphasized for the non-tubular geometry if it is compared with the tubular one (especially in the case of tapered adherends).

The stability of brittle crack propagation and the size effects on mechanical collapse behaviour, as well as the ductile-brittle transition are emphasized. Some experimental results obtained with non-tubular joints agree satisfactorily with the theory herein presented.

PRINCIPLE OF ENERGY CONSERVATION

By virtue of the Principle of Conservation of Energy, the following balance between the variation in the potential energy and the virtual fracture energy must hold:

$$\mathcal{G}\,\mathrm{d}A + \mathrm{d}W = 0 \tag{1}$$

where $\mathcal{G}$ is the strain energy release rate and $\mathrm{d}A$ represents the incremental fracture area.

Considering an imposed torsional loading, the variation in the potential energy is equal to:

$$\mathrm{d}W = \mathrm{d}L - M_t\,\mathrm{d}\vartheta = \mathrm{d}\left(\frac{1}{2}M_t\vartheta\right) - M_t\,\mathrm{d}\vartheta = -\mathrm{d}L \tag{2}$$

where $\mathrm{d}L$ denotes the variation in elastic strain energy (evaluated by virtue of Clapeyron's Theorem). The strain energy release rate can be rewritten as:

$$\mathcal{G} = -\frac{\mathrm{d}W}{\mathrm{d}A} = \frac{\mathrm{d}L}{\mathrm{d}A} \tag{3}$$

Brittle crack propagation really occurs when $\mathcal{G}$ reaches its critical value $\mathcal{G}_a$, characteristic for the adhesive:

$$\mathcal{G} = \frac{\mathrm{d}L}{\mathrm{d}A} = \mathcal{G}_a \tag{4}$$

and such propagation will be stable, metastable or unstable depending on the sign of the second order derivative of total potential energy:

$$-\frac{\mathrm{d}^2W}{\mathrm{d}A^2} = \frac{\mathrm{d}\mathcal{G}}{\mathrm{d}A} = \frac{\mathrm{d}^2L}{\mathrm{d}A^2}\begin{cases} <0 & \textit{stable} \\ =0 & \textit{metastable} \\ >0 & \textit{unstable} \end{cases} \tag{5}$$

NON-TUBULAR BONDED JOINT

The nontubular bonded joint (Fig. 1), consisting of two elements and the interposed adhesive, is considered to be subject to a torsional moment M_t. The theoretical analysis[4,6] permits the calculation of the torsional moment M absorbed by each beam in each section of the overlap and the predominant normal strain ε_y and normal stress σ_y fields (equivalent to the applied torsional moment) in the adhesive:

$$M_i(x) = M_t f_i(x); \quad f_1(x) + f_2(x) = 1;$$
$$\begin{cases} f_1(x = -c) = 1 \\ f_1(x = +c) = 0 \end{cases}; \quad i = 1, 2 \tag{6}$$

$$\sigma_y(x, z) = -\frac{M_t}{I_x^*} z \frac{\mathrm{d}f_1(x)}{\mathrm{d}x} = E_a^* \varepsilon_y(x, z);$$
$$E_a^* = \frac{1 - \nu_a}{(1 + \nu_a)(1 - 2\nu_a)} E_a; \quad I_x^* = \frac{b^3}{12} \tag{7}$$

where f are known functions, I_x^* is a moment of inertia per unit length and E_a, ν_a are the Young's modulus and the Poisson's ratio of the adhesive. The predominant stress field $\sigma_y(x, z)$ in the adhesive is linear along the z-axis and its maximum positive value is achieved at $z = b/2$. It is supposed that the initial separation at the interface between the two adherends takes place in the adhesive in $z = b/2$, the zone of highest stress concentration, with a crack of length Δz for all the length $2c$ of the overlap (Fig. 2).

We can suppose that the fictitious cross length of the joint becomes $b - \Delta z$. This is the simplest hypothesis: the stiffness of the joint is linear in Δz. If the crack length is zero it will coincide with the stiffness of the integral joint and if the crack length is equal to b it will be equal to zero. By this hypothesis good predictions of the failure loads of the joint can be obtained.

The elastic strain energy of the overlap zone of the joint is the sum of three quantities, i.e. the elastic strain

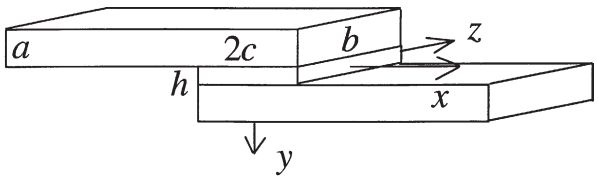

Fig. 1 Non-tubular bonded joint.

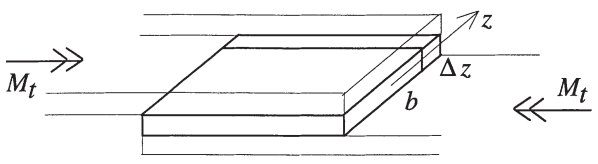

Fig. 2 Debonding in the adhesive of a non-tubular joint.

energy absorbed by the two beams (subscript 1, 2) and by the adhesive (subscript 3):

$$L = L_1 + L_2 + L_3 \tag{8}$$

If we consider a beam with tapered adherends along the overlap zone of a cracked joint, the fictitious factor of torsional rigidity $I_i^f(x)$ can be written as a function of the profile $a_i^3(x) = a_i^3 h_i(x)$, where a_i, I_i are the height and the factor of torsional rigidity of the considered beam out of the overlap zone:

$$I_i^f(x) = 1/3 a_i^3(x)(b - \Delta z) = I_i h_i(x)(1 - \Delta z/b) \tag{9}$$

The elastic strain energy absorbed by the beam along the overlap zone of the cracked joint is equal to:

$$L_i = \int_{-c}^{+c} \frac{M_i^2(x)}{2G_i I_i^f(x)}\,\mathrm{d}x = \frac{M_i^2}{2G_i I_i}\,\frac{1}{1 - \Delta z/b}\int_{-c}^{+c}\frac{f_i^2(x)}{h_i(x)}\,\mathrm{d}x$$
$$= \frac{M_t^2}{2G_i I_i}\,\alpha_i(\Delta z); \quad i = 1, 2 \tag{10}$$

where α_i are integrals of known functions.[4]

The elastic strain energy absorbed by the adhesive of the cracked joint can be written as a function of the fictitious moment of inertia per unit length, $I_x^{*f} = (b - \Delta z)^3/12$, considering the reduction of the load-bearing area of the adhesive in the stress fields [Eq. (7)]:

$$L_3 = \int_{-c}^{+c}\int_{-(b-\Delta z)/2}^{+(b-\Delta z)/2}\frac{1}{2}E_\mathrm{a}\varepsilon_y^2(x, z)h\,\mathrm{d}z\,\mathrm{d}x$$
$$= \frac{2 - 6\nu_\mathrm{a} + 3\nu_\mathrm{a}^2 + 2\nu_\mathrm{a}^3}{\nu_\mathrm{a}^2 E_\mathrm{a}}\,\frac{6hM_t^2}{b^3}$$
$$\times \frac{1}{(1 - \Delta z/b)^3}\int_{-c}^{+c}\left(\frac{\mathrm{d}f_1(x)}{\mathrm{d}x}\right)^2\mathrm{d}x$$
$$= \frac{M_t^2}{2K_\mathrm{a}}\,\beta(\Delta z) \tag{11}$$

where b, K_a are, respectively, the height and the stiffness of the adhesive and β is the integral of a known function.[4] Applying Eq. (3) we can obtain the strain energy release rate $\mathcal{G}$ where $\mathrm{d}A = 2c\,\mathrm{d}\Delta z$. Equation (5) shows whether the fracture propagation is stable, metastable or unstable, for a non-tubular joint. By Eq. (4) we can obtain the condition for brittle propagation:

$$\frac{M_t^2 b/2}{A_\mathrm{a}}\left(\frac{\dot{\alpha}_1}{G_1 I_1} + \frac{\dot{\alpha}_2}{G_2 I_2} + \frac{\dot{\beta}}{K_\mathrm{a}}\right) = \mathcal{G}_\mathrm{a} \tag{12}$$

where the dot over the symbol has the meaning of derivative with respect to the crack length Δz.

The derivatives in Eq. (12) depend on the ratio between the effective load-bearing bonded area $A_\mathrm{a}^\mathrm{eff}$ of the adhesive surface and its nominal value $A_\mathrm{a} = 2bc$. It can be expressed as a function of the initial crack length:

$$\frac{A_\mathrm{a}^\mathrm{eff}}{A_\mathrm{a}} = 1 - \frac{\Delta z}{b} \tag{13}$$

and depends on the technological process of bonding. If the process is *perfect* it equals one. From Eq. (12) we can obtain the torsional moment causing the brittle collapse of the joint.

TUBULAR BONDED JOINT

The same considerations can be rewritten taking into account a tubular bonded joint.[7] In this case the predominant stress and strain fields [Eq. (7)] become:

$$\tau(x) = -\frac{M_t}{2\pi R^2}\,\frac{\mathrm{d}f_1(x)}{\mathrm{d}x} = G_\mathrm{a}\gamma(x) \tag{14}$$

where R is the radius of the bonded surface and G_a is the shear elastic modulus of the adhesive.

It is well-known that the predominant shearing stress field in the adhesive (equivalent to the applied torsional moment) has its maximum positive value at the end of the stiffer beam (here called 1). The initial separation at the interface between the two adherends is supposed to take place at this point: the debond is a crown-crack of length Δx (Fig. 3). The elastic strain energy of the cracked (eventually tapered) joint along the overlap can be calculated, noting how the portions of the joint are loaded (Fig. 3):

$$L_1 = \int_{-c}^{+c-\Delta x}\frac{M_1^2(x)}{2G_1 I_1(x)}\,\mathrm{d}x = \frac{M_t^2}{2G_1 I_1}\int_{-c}^{+c-\Delta x}\frac{f_1^2(x)}{h_1(x)}\,\mathrm{d}x$$
$$= \frac{M_t^2}{2G_1 I_1}\,\alpha_1(\Delta x) \tag{15}$$

$$L_2 = \int_{-c}^{+c-\Delta x}\frac{M_2^2(x)}{2G_2 I_2(x)}\,\mathrm{d}x + \int_{+c-\Delta x}^{+c}\frac{M_t^2}{2G_2 I_2(x)}\,dx$$
$$= \frac{M_t^2}{2G_2 I_2}\,\alpha_2(\Delta x) + \frac{M_t^2}{2G_2 I_2}\,\alpha_2^*(\Delta x) \tag{16}$$

where α_i, α_2^*, I_i are, respectively, integrals of known functions[7] depending on the crack length Δx and on the polar moment of inertia out of the overlap zone for the considered beam.

The elastic strain energy absorbed by the adhesive of the cracked joint is equal to:

$$L_3 = \int_{-(2c-\Delta x)/2}^{+(2c-\Delta x)/2}\frac{1}{2}G_\mathrm{a}\gamma^2(x)2\pi Rh\,\mathrm{d}x$$
$$= \frac{hM_t^2}{4\pi R^3 G_\mathrm{a}}\int_{-(2c-\Delta x)/2}^{+(2c-\Delta x)/2}\left(\frac{\mathrm{d}f_1(x)}{\mathrm{d}x}\right)^2\mathrm{d}x$$
$$= \frac{M_t}{2K_\mathrm{a}}\,\beta(\Delta x) \tag{17}$$

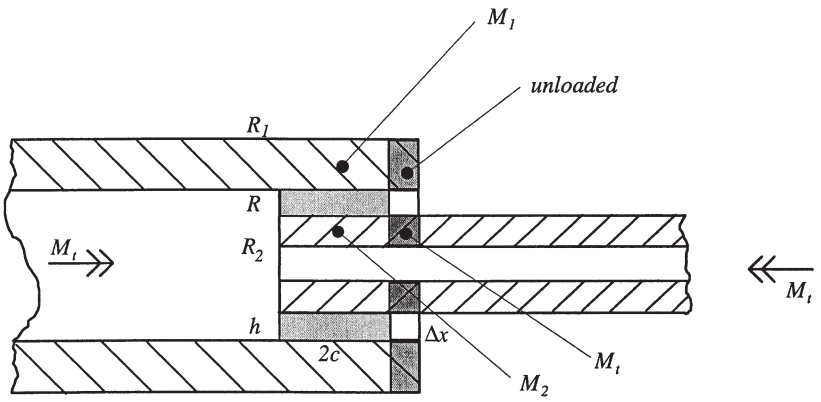

Fig. 3 Tubular bonded joint with debonding in the adhesive.

where β is the integral of a known function[7] depending on the crack length Δx. Applying Eq. (3) we can obtain the strain energy release rate $\mathcal{G}$ where $\mathrm{d}A = 2\pi R\,\mathrm{d}\Delta x$. Equation (5) shows whether the fracture propagation is stable, metastable or unstable, for a tubular joint.

By Eq. (4) the condition for brittle propagation can be obtained as:

$$\frac{M_t^2 c}{A_a}\left(\frac{\dot{\alpha}_1}{G_1 I_1} + \frac{\dot{\alpha}_2 + \dot{\alpha}_2^*}{G_2 I_2} + \frac{\dot{\beta}}{K_a}\right) = \mathcal{G}_a \tag{18}$$

where the dot over the symbol has the meaning of derivative with respect to the crack length Δx, and $A_a = 4\pi Rc$ is the area of the adhesive surface.

STABILITY OF CRACK PROPAGATION

If we suppose that the height h of the adhesive layer is zero (and as a consequence $L_3 = 0$), the functions f will assume the physical meaning of coefficients of distribution:

$$f_i(x) = \frac{G_i I_i(x)}{G_1 I_1(x) + G_2 I_2(x)}; \quad -c < x < c \tag{19}$$

Two cases are particularly interesting. In the case of non-tapered adherends, the functions [Eq. (19)] are constant along x ($x \neq \pm c$) and Eqs (12) and (18) can be rewritten in the following unified manner:

$$M_t = \sqrt{\mathcal{G}_a \frac{A_a}{c}\gamma(G_1 I_1 + G_2 I_2)};$$

$$\begin{cases} \gamma = \left(\dfrac{A_a^{\mathrm{eff}}}{A_a}\right)^2; \quad \gamma \leqslant 1; \quad \textit{non-tubular}, \quad \textit{unstable} \\ \gamma = \dfrac{G_2 I_2}{G_1 I_1}; \quad \gamma \leqslant 1; \quad \textit{tubular}, \quad \textit{metastable} \end{cases} \tag{20}$$

The stability of crack propagation has been obtained applying Eq. (5). For non-tubular joints an increase of crack length causes a reduction in the torsional moment of brittle failure: the propagation will be unstable. For tubular joints the torsional moment of brittle failure is independent of the crack length: the propagation will be metastable.

Equation (5) has been already presented and verified experimentally in the work by Gent and Yeoh[8] for tubular joints in the case of $G_1 I_1 \to \infty$. In that paper a better estimate of the torsional moment, considering the frictional contribution to the work of detachment due to the shrinking of a tube subjected to torsion, is also presented. Such a frictional effect cannot be neglected except in the case when the external tube is much stiffer than the internal one, and in any case it vanishes for non-tubular joints.

In the case of tapered adherends of beams with identical stiffness GI, we can consider the following approximated profile:

$$G_1 I_1(x) = GI\frac{c + x}{2c}; \quad G_2 I_2(x) = GI\frac{c - x}{2c} \tag{21}$$

This profile is the best from a tension point of view (*Uts* Joints, i.e. optimized to Uniform Torsional Strength; Refs [6,7]). In this case Eqs (15) and (16) must be rewritten taking into account the symmetrical propagation by the length $\Delta x/2$ of the crack at the end of the two beams:

$$\begin{aligned} L_1 &= \int_{-c+\Delta x/2}^{+c-\Delta x/2} \frac{M_1^2(x)}{2G_1 I_1(x)}\,\mathrm{d}x + \int_{-c}^{-c+\Delta x/2} \frac{M_t^2}{2G_1 I_1(x)}\,\mathrm{d}x \\ &= L_2 = \int_{-c+\Delta x/2}^{+c-\Delta x/2} \frac{M_2^2(x)}{2G_2 I_2(x)}\,\mathrm{d}x + \int_{+c-\Delta x/2}^{+c} \frac{M_t^2}{2G_2 I_2(x)}\,\mathrm{d}x \end{aligned} \tag{22}$$

Equation (20) becomes:

$$M_t = \sqrt{\mathcal{G}_a \frac{A_a}{c}\gamma GI};$$

$$\begin{cases} \gamma = \left(\dfrac{A_a^{\mathrm{eff}}}{A_a}\right)^2; \quad \gamma \leqslant 1; \quad \textit{non-tubular (uts)}, \textit{ unstable} \\ \gamma = \dfrac{A_a + A_a^{\mathrm{eff}}}{A_a - A_a^{\mathrm{eff}}}; \quad \gamma \geqslant 1; \quad \textit{tubular (uts)}, \textit{ unstable} \end{cases} \tag{23}$$

For tubular or non-tubular joints with (*uts*) tapered adherends an increase in the crack length causes a reduction in the torsional moment of brittle failure: the propagation will be unstable.

According to Eq. (23) it appears very clear that the non-tubular joint is more susceptible to brittle collapse than the tubular one.

The non-tubular tapered joints are less strong than the non-tapered ones from a brittle fracture point of view. If the full benefits of the *uts* non-tubular joint geometry are to be exploited, it is thus essential for appropriate technological purposes to ensure that the joint collapse does not involve fracture phenomena.

Vice-versa, the tubular tapered joint is stronger than the non-tapered one against brittle collapse. As a consequence the *uts* tubular joint is optimized at the same time from a ductile and a brittle point of view; this is a relevant result for a global optimization design.

SIZE EFFECTS AND DUCTILE–BRITTLE TRANSITION

The critical torsional moment is provided by the lesser of the load of brittle crack propagation [Eqs (20) and (23)] and the load of ductile collapse achieved when the maximum stress in the adhesive equals an ultimate stress $\sigma_u = \tau_\mu \sqrt{3}$[4,6,7]

$$M_t^\sigma = \sqrt{\frac{A_{ac}}{G_a}\lambda\frac{G_2 I_2}{G_1 I_1}(G_1 I_1 + G_2 I_2)}\,\tau_u, \quad \frac{G_2 I_2}{G_1 I_1} \leqslant 1,$$

$$\begin{cases} \lambda = \left(\dfrac{A_a^{eff}}{A_a}\right)^2 \dfrac{1-2\nu_a}{2-2\nu_a}; & \textit{non-tubular} \\ \lambda = 1; & \textit{tubular} \end{cases} \tag{24}$$

$$M_t^\sigma = \begin{cases} \dfrac{\sqrt{3}}{3}\left(\dfrac{A_a^{eff}}{A_a}\right)^2 b^2 c\tau_u; & \textit{non-tubular (uts)} \\ 4\pi R^2 \dfrac{A_a^{eff}}{A_a} c\tau_u; & \textit{tubular (uts)} \end{cases} \tag{25}$$

where A_{ac} is the cross-section area of the adhesive layer (bh or $2\pi Rh$ for non-tubular or tubular joints, respectively).

Comparing the ultimate values of the torsional moment for brittle [Eqs (20) and (23)] and ductile collapse [Eqs (24) and (25)] the brittleness number s of the joint may be defined:[10,12]

$$\frac{M_t}{M_t^\sigma} = \mu s; \quad \begin{cases} \mu = 2\left(\dfrac{a_1}{h}\right)^{3/2}\left(\dfrac{h}{a_2}\right)^{3/2}; \quad s = \sqrt{\dfrac{G_1}{G_2}\dfrac{1-\nu_a}{1-2\nu_a}}\dfrac{\sqrt{\mathcal{G}_a G_a}}{\sqrt{h}\tau_u}; & \textit{non-tubular} \\ \mu = \sqrt{2}; \quad s = \dfrac{\sqrt{\mathcal{G}_a G_a}}{\sqrt{h}\tau_u}; & \textit{tubular} \\ \mu = \sqrt{2}\left(\dfrac{a_i}{h}\right)^{3/2}\dfrac{b}{b}\dfrac{h}{c}\dfrac{A_a}{A_a^{eff}}; \quad s = \dfrac{\sqrt{\mathcal{G}_a G_i}}{\sqrt{h}\tau_u}, \quad i = 1 \textit{ or } 2; & \textit{non-tubular (uts)} \\ \mu = \dfrac{\sqrt{8}}{8}\sqrt{\left|\dfrac{R_i^4}{h^4} - \dfrac{R^4}{h^4}\right|\dfrac{A_a + A_a^{eff}}{A_a - A_a^{eff}}}; \quad s = \dfrac{\sqrt{\mathcal{G}_a G_i}}{\sqrt{h}\tau_u}, \quad i = 1 \textit{ or } 2; & \textit{tubular (uts)} \end{cases} \tag{26}$$

Considering different sizes of geometrically similar joints (μ = const.) the brittleness number s shows how brittle collapses tend to occur with a low fracture energy, a low shear elastic modulus, a high ultimate stress and/or large structural sizes. It is not their individual values that are responsible for the nature of the collapse mechanism, but rather their continued effect as represented by the function s.

EXPERIMENTAL ASSESSMENT

To validate the theory to predict the brittle collapse of bonded joints, some experimental tests have been carried out by the Fiat Research Centre.[17] The typologies considered are non-tubular, without tapered adherends (specimens A) with two different cross sections (A1: b = 37.5 mm, A2: b = 25 mm) or with trapezoidal tapered adherends (specimens B with b = 37.5 mm, Fig. 4). Three tests (displacement controlled with deformation rate variable between 2 and 5 mm/min) for each one of the three typologies for a total of nine cases have been considered.

The room temperature and humidity were, respectively, 22 °C and 50% (relative humidity).

The material of the beams is magnesium (E = 45 GPa, ν = 0.31), and the adhesive is epoxy CIBA XB 5315 (E_a = 2.7 GPa, ν_a = 0.4). The experimental set-up is represented in Fig. 5 and the geometrical values are reported in Table 1. Table 2 shows the experimental results.

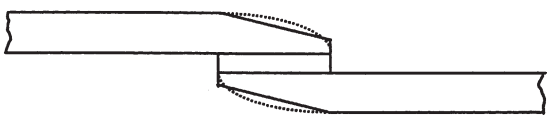

Fig. 4 Trapezoidal execution of non-tubular tapered profile (continuous line) and *uts* one (dotted line).

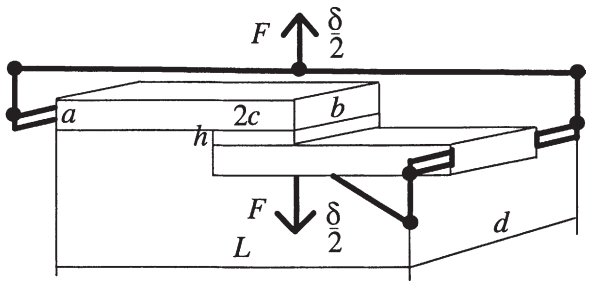

Fig. 5 Testing set-up for torsion tests.

Table 1 Geometrical sizes [mm]

a	*b*	*c*	*h*	*d*	*L*
3	3.75–25	10	0.3	94	150

Table 2 Experimental results for the loading capacity *F* (N)

A1	118	168	—
A2	84	112	126
B	115	123	168

The variability of the results considering the same joint is a consequence of the difficulty of execution a bonding with constant properties. For this reason a discrepancy between the theoretical and experimental analysis is unavoidable and expected (see Ref. [8]).

The unstable phenomenon appeared experimentally in a very clear way.

In Fig. 6 the two kinds of joint tested are presented. A better distribution of adhesive between the two adherends at the end of the test implies a higher value of A_a^{eff}/A_a. The mean value of this ratio is experimentally around 0.7 and can be used to model a real and imperfect bonding.

Referring to Fig. 5, the torsional moment applied and the relative rotation can be calculated as:

$$M_t = \frac{F}{2} d; \quad \Delta\vartheta = 2\text{arctg}\left(\frac{\delta}{d}\right) \tag{27}$$

and it is possible to obtain a relation between these two quantities for each test. In Fig. 7, to provide some examples, these curves for specimens B are reported. The fracture energy of the adhesive epoxy can be estimated around 140 Jm^{-2}.[8,18]

Considering a perfect or an imperfect bonding

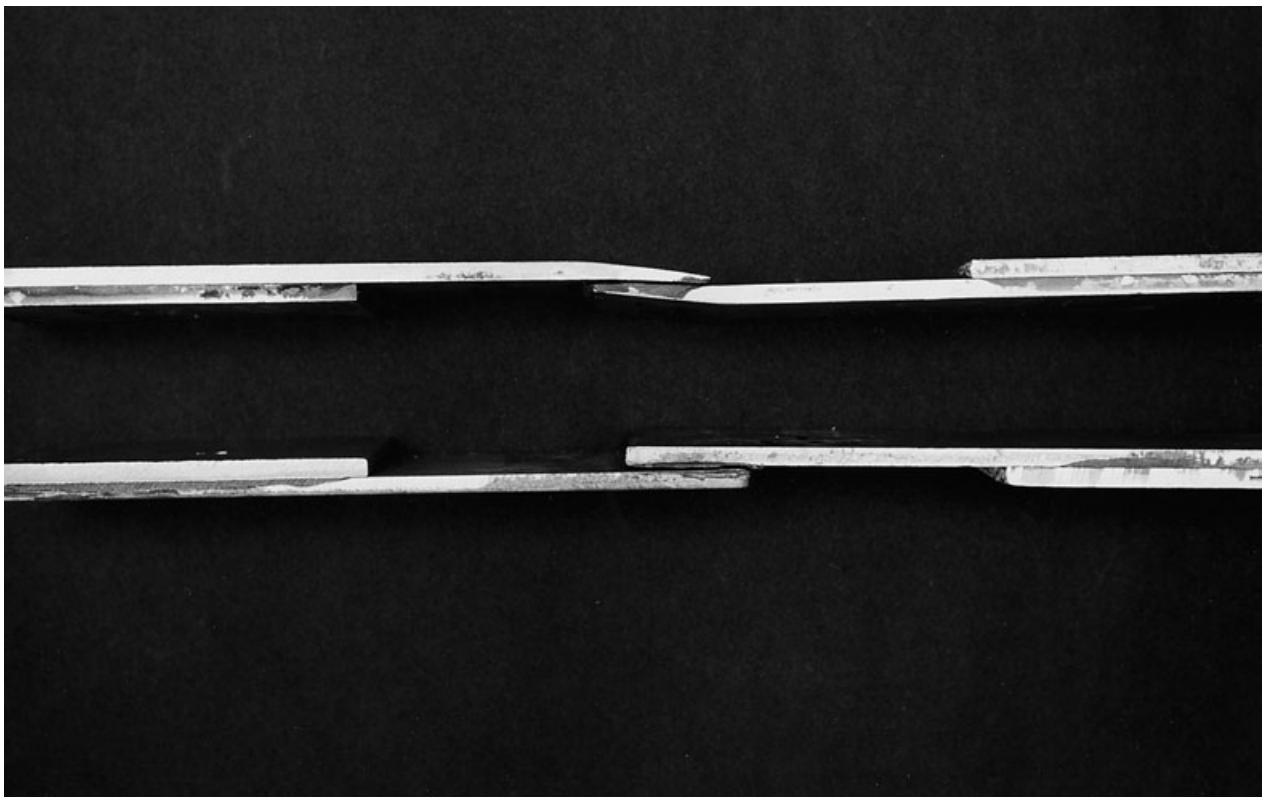

Fig. 6 Bonded joints with and without tapered adherends.

Table 3 Theoretical predictions with perfect or imperfect bonding ($A_a^{eff}/A_a = 1.0$ or 0.7, respectively) and experimental results for the torsional moment of failure [Nm]

Joint	Theoretical (ideal joint) $A_a^{eff}/A_a = 1$	Theoretical (real joint) $A_a^{eff}/A_a = 0.7$	Experimental values			Experimental average value
A1	11.00	7.70	5.55	7.90	—	6.72
A2	7.82	5.47	3.95	5.27	5.93	5.04
B ($\approx$ *uts* profile)	7.29	5.10	5.40	5.78	7.90	6.36

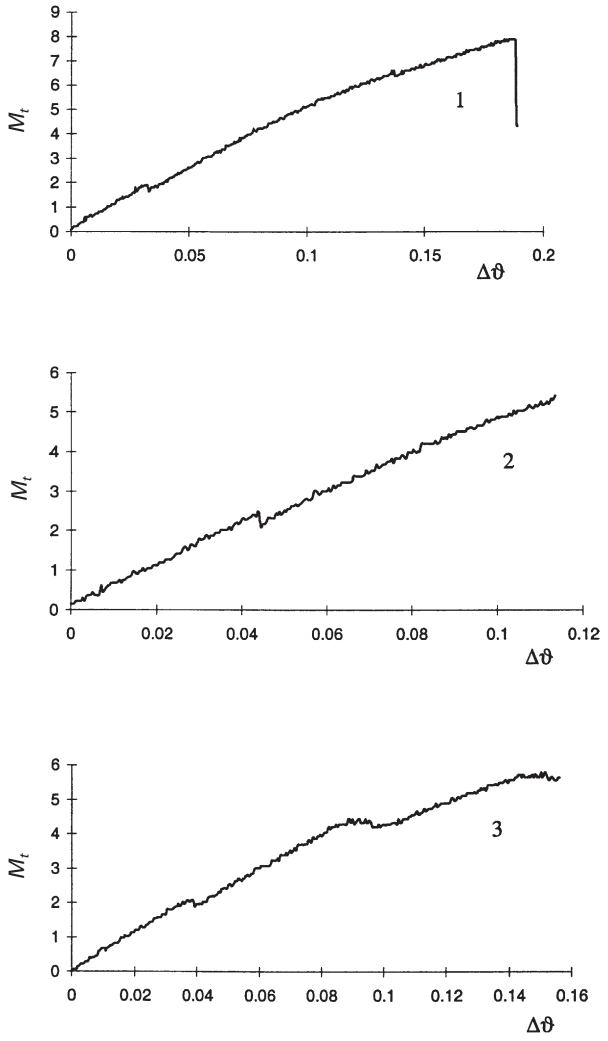

Fig. 7 Experimental diagrams of torsional moment [Nm] versus relative rotation (rad) for the specimens B.

($A_a^{eff}/A_a = 1.0$ or 0.7, respectively) and using Eq. (20), we can predict the critical value of the torsional moment for the specimens A1, A2 tested.

Using the analytical *uts* profiles Eq. (21) to approximate the experimental trapezoidal tapered adherend profiles (Fig. 4), we can estimate using Eq. (23) the critical value of the torsional moment for the specimens B that were tested. In these cases brittle crack propagation precedes ductile collapse, since the ratio expressed by Eq. (26) is less than one. The comparison is summarized in Table 3; the theoretical ('real joint' column) and the experimental ('average value' column) results agree satisfactorily. As a consequence, the prediction of Eqs (20) and (23), obtained supposing an imperfect bonding, can be used as estimate of the torsional moment of failure of the joint. On the other hand, considering a perfect bonding ('ideal joint' column in Table 3), the prediction of Eqs (20) and (23) will be an upper-bound value for the torsional moment of failure concerning a particular type of joint ('experimental values' columns).

CONCLUSIONS

In this paper a simple Griffith fracture energy criterion to predict the brittle failure load for tubular or non-tubular bonded joints subjected to torsion has been described [see Eq. (20)].

The tapering of the adherends has also been investigated. It has been shown as the *uts* profile [Eq. (21)], optimizing the joint from a tension point of view, also implies a decrease of the brittleness of the tubular joint [see Eq. (23)]. As a consequence the *uts* tubular joint is optimized at the same time from a ductile and a brittle point of view; this is a relevant result for a global optimization design.

The stability of brittle crack propagation and the size effects on mechanical collapse behaviour, as well as the ductile-brittle transition, has also been investigated. The greater sensitivity to brittle collapse is emphasized for the non-tubular geometry if it is compared with the tubular one (especially in the case of tapered adherends).

Finally, experimental measurements of failure loads under torsion for non-tubular bonded joints have been presented; they agree satisfactorily with the theoretical predictions.

Acknowledgements

The authors gratefully acknowledge Fiat Research Centre (CRF) for providing the experimental results reported in the present paper.

The present research was carried out with the financial support of the Ministry of University and Scientific Research (MURST), the National Research Council

(CNR) and the EC-TMR Contract N° ERBFMRXCT960062.

REFERENCES

1 Goland, M. and Reissner, E. (1944) The stresses in cemented joints. *J. Appl. Mech.* **11,** 17–27.
2 Lubkin, J. L. and Reissner, E. (1956) Stress distribution and design data for adhesive lap joints between circular tubes. *Trans. ASME* **78,** 1213–1221.
3 Adams, R. D. and Peppiatt, N. A. (1977) Stress analysis of adhesive bonded tubular lap joints. *J. Adhesion* **9,** 1–18.
4 Pugno, N. and Surace, G. (2000) Non-tubular bonded joint under torsion: Theory and numerical validation. *Struct. Engng Mech.* **10,** 125–138.
5 Pugno, N. (2001) Closed form solution for a non-tubular bonded joint with tapered adherends under torsion. *Int. J. Mech. Control* **2,** 19–27.
6 Pugno, N. (1999) Optimising a non-tubular adhesive bonded joint for uniform torsional strength. *Int. J. Mater. Product Technol.* **14,** 476–487.
7 Pugno, N. and Surace, G. (2001) Tubular bonded joint under torsion: analysis and optimization for uniform torsional strength. *J. Strain Anal. Engng Design* **1,** 17–24.
8 Gent, A. N. and Yeoh, O. H. (1982) Failure loads for model adhesive joints subjected to tension, compression or torsion. *J. Mater. Sci.* **17,** 1713–1722.
9 Griffith, A. A. (1921) The phenomena of rupture and flow in solids. *Phil. Trans. Royal Soc.* **A221,** 163–198.
10 Carpinteri, A. (1981) Static and energetic fracture parameters for rocks and concretes. *Mater. Struct.* **14,** 151–162.
11 Carpinteri, A. (1984) Interpretation of Griffith instability as a bifurcation of the global equilibrium. In: *NATO Advanced Research Workshop on Applications of Fracture Mechanics to Cementitious Composites*, pp. 287–316.
12 Carpinteri, A. (1989a) Cusp catastrophe interpretation of fracture instability. *J. Mech. Physics Solids* **37,** 567–582.
13 Carpinteri, A. (1989b) Decrease of apparent tensile and bending strength with specimen size: two different explanations based on fracture mechanics. *Int. J. Solids Struct.* **25,** 407–429.
14 Carpinteri, A. (1989c) Size effects on strength, toughness and ductility. *J. Engng Mech.* **115,** 1375–1392.
15 Carpinteri, A. (1989d) Softening and snap-back instability in choesive solids. *Int. J. Numer Meth Engng* **28,** 1521–1537.
16 Carpinteri, A. (1997) *Structural Mechanics—A Unified Approach*. E&FN Spon, London.
17 Pugno, N. (1998) *Non Tubular Bonded Joints Under Torsion*, Ph.D. Thesis. Department of Structural Engineering, Politecnico di Torino, Torino, Italy.
18 Moloney, A. C., Kausch, H. H. and Stieger, H. R. (1984) The use of the double torsion test geometry to study the fracture of adhesive joints. *J. Mater. Sci. Lett.* **3,** 776–778.